INTERNATIONAL JOURNAL FOR NUMERICAL AND ANALYTICAL METHODS IN GEOMECHANICS
Int. J. Numer. Anal. Meth. Geomech., **23**, 577–594 (1999)

POROELASTIC-PLASTIC CONSOLIDATION — ANALYTICAL SOLUTION

W. G. PARISEAU*

Department of Mining Engineering, University of Utah, 135 So. 1460 East, Rm 315, Salt Lake City, UT 84112-0013, U.S.A.

SUMMARY

Consolidation of a poroelastic material that yields according to Drucker–Prager or Mohr–Coulomb criteria leads to a Stefan problem for time-dependent pore fluid pressure. The solution to the Stefan problem for a column of infinite depth is known and is adapted to poroelastic/plastic consolidation of a weightless material under a uniform surface load applied instantaneously and subsequently maintained constant. In this approach, the plastic potential and yield criterion need not be the same. If yielding occurs concurrently with application of load, then collapse is instantaneous. Otherwise, yielding may occur during the consolidation period. If so, then the elastic–plastic zone first appears at the surface and subsequently moves down the column. Depth to the elastic–plastic boundary is given by the simple expression $Z = 2\beta\sqrt{t}$ where β is a constant determined from continuity conditions at the elastic–plastic boundary. Time-dependent surface displacement that occurs during consolidation is directly proportional to Z. There is little difference between elastic–plastic and purely elastic results in a numerical example because there is little difference in the respective consolidation coefficients. Elastic–plastic finite element results obtained from a column of finite depth are in close agreement with analytical results as long as the pore pressure at the bottom of the column does not change significantly from the value induced by application of the surface load. The analytical solution provides for: (1) efficient evaluation of material properties effects on consolidation, including strength and fluid compressibility, and (2) an accurate way of validating poroelastic/plastic computer codes that are based on Drucker–Prager and Mohr–Coulomb criteria.

Key words: poroelasticity; plasticity; consolidation

INTRODUCTION

Consolidation of a saturated porous solid under a uniform, constant load is an interesting poroelastic/plastic problem for several reasons including the fact that an analytic solution is possible using Drucker–Prager and Mohr–Coulomb failure criteria. In this regard, consolidation of a weightless column of finite depth in the purely elastic range of response is well-known, e.g. References 1 and 2, and often used for poroelastic finite element code validation.[3,4] A comprehensive review of poroelasticity is provided by Detournay and Cheng.[5] Solution to elastic consolidation under self-weight is discussed by Pariseau.[6] The two cases are illustrated in

* Correspondence to: W. G. Pariseau, Department of Mining Engineering, University of Utah, 135 S. 1460 East, Room 315, Salt Lake City, UT 84112-0013, U.S.A.

Contract grant sponsor: Department of Interior's Mineral Institute Program administered by the Bureau of Mines through the Generic Minerals Technology Center in Mine Systems Design and Ground Control; contract grant number: G1145251.

CCC 0363–9061/99/070577–18$17.50

Received 10 December 1997
Revised 14 May 1998

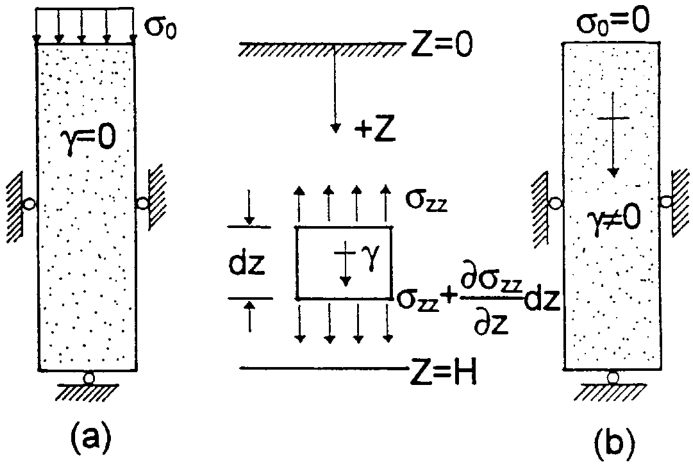

Figure 1. Consolidation: (a) weightless material under a uniform surface load; (b) under material weight only

Figure 1. In both cases, the total vertical stress at any depth is independent of time. This feature is easily recognized in consideration of equilibrium in the vertical direction. The result is an uncoupling of solid deformation and fluid flow; fluid stress is then governed by a diffusion equation. The form of the diffusion equation is the same in the elastic and elastic–plastic domains, but the diffusion coefficient is different. The situation leads to a classic Stefan problem in the case of an infinitely deep column or half-space.

The immediate problem objectives are to calculate the fluid stress and velocity, solid stress and strain, and displacement fields as functions of time. The purpose is to provide a reliable way of verifying poroelastic/plastic finite element codes. In this regard, no analytical solutions have been found in the technical literature. Computer model verification has necessarily relied on comparisons with other numerical results that are often of uncertain accuracy. Thus, while the problem of one-dimensional poroelastic/plastic consolidation (uniaxial strain) may not be of great practical importance, the results may be of some aid to the establishment of computer code reliability. There is also some interest in examining the effect of strength and inelastic deformation on the consolidation process even within the confines of classical plasticity theory for geologic media.

GOVERNING EQUATIONS

The governing equations follow from specialization of equilibrium requirements, kinematics and material laws. Elastic–plastic deformation and boundary conditions at the column top and the elastic–plastic interface between are of particular interest.

Total stress required for equilibrium is considered to be the sum

$$\sigma_{zz} = \sigma'_{zz} + \pi \tag{1}$$

where σ'_{zz} is the effective (solid) stress and π is the fluid contribution (effective fluid stress) to the total stress; *tension is considered positive for solid and fluid stress.* The effective fluid stress is related to fluid pressure of magnitude p measured by a gauge connected to the fluid-filled void space, that

is, $\pi = -\alpha p$ where α is material constant, generally considered to a have a numerical value between porosity and unity; $\alpha = 1$ is a common choice in soil mechanics.

The equilibrium requirement for total vertical stress is

$$\frac{\partial \sigma_{zz}}{\partial z} + \gamma = 0 \tag{2}$$

where γ is the saturated specific weight of the material. Equilibrium of the fluid requires

$$\frac{\partial \pi}{\partial z} + \gamma_{\mathrm{f}} = R \tag{3}$$

where γ_{f} is a specific weight of fluid (weight per unit total volume) and R is resistance to flow caused by viscous drag between fluid and solid particles. However, the idealized fluid is non-viscous.

The velocity of the fluid relative to the solid is given by Darcy's law

$$\frac{\partial \omega}{\partial t} = k\left(\frac{\partial \pi}{\partial z} + \gamma_{\mathrm{f}}\right) \tag{4}$$

where k is hydraulic conductivity and isotropy is implied; ω is the relative displacement between fluid and solid. In view of (3), $R = (\partial\omega/\partial t)/k$ as usual.

In the range of purely elastic deformation, the stress strain relations in incremental form follow from Hooke's law and the concept of effective stress. Thus, under complete lateral restraint, indicated in Figure 1,

$$\begin{aligned} 0 &= \mathrm{d}\sigma'_{xx} - \nu \mathrm{d}\sigma'_{yy} - \nu \mathrm{d}\sigma'_{zz} \\ 0 &= \mathrm{d}\sigma'_{yy} - \nu \mathrm{d}\sigma'_{xx} - \nu \mathrm{d}\sigma'_{zz} \\ E\mathrm{d}\varepsilon^{\mathrm{s}}_{zz} &= \mathrm{d}\sigma'_{zz} - \nu \mathrm{d}\sigma'_{yy} - \nu \mathrm{d}\sigma'_{xx} \end{aligned} \tag{5}$$

where E and ν are Young's modulus and Poisson's ratio, respectively. Equations (5) imply $\mathrm{d}\varepsilon^{\mathrm{s}}_{zz} = \mathrm{d}\sigma'_{zz}/E'$, where

$$E' = E_{\mathrm{e}} = \frac{E(1-\nu)}{[(1+\nu)(1-2\nu)]} \tag{5b}$$

is an 'effective' elastic deformation modulus, so $\varepsilon^{\mathrm{s}}_{zz} = \sigma'_{zz}/E' + \varepsilon^{\mathrm{s}}_0$, ($\varepsilon^{\mathrm{s}}_0$ is an initial strain).

The deformation of the fluid, which lacks viscosity, is always elastic and reflected in the fluid volumetric strain: $e^{\mathrm{f}} = c\pi$ where c is the fluid compressibility. The four independent poroelastic constants are therefore α, E, ν and c. Volumetric strain of the fluid relative to the solid is the difference $e^{\mathrm{f}} - e^{\mathrm{s}}$, so

$$\frac{\partial \omega}{\partial z} = c\pi - \left(\frac{\sigma'_{zz}}{E'} + \varepsilon^{\mathrm{s}}_0\right) \tag{6}$$

Hence

$$\frac{\partial^2 \omega}{\partial z \partial t} = c\,\frac{\partial \pi}{\partial t} - \left(\frac{1}{E'}\right)\left(\frac{\partial \sigma_{zz}}{\partial t} - \frac{\partial \pi}{\partial t}\right) \tag{7}$$

where use is made of equation (1). But also from equation (4)

$$\frac{\partial^2\omega}{\partial t\partial z} = k\,\frac{\partial^2\pi}{\partial z^2} \tag{8}$$

where specific weight of the fluid is considered constant.

In the case of a weightless material settling under a constant compressive surface load $-\sigma_0$, the total stress at the surface is constant, so $\partial\sigma_{zz}/\partial t = 0$. In the absence of an applied load at the surface (which could be a tension), but in consideration of weight, $\partial\sigma_{zz}/\partial z = -\gamma$, so $\sigma_{zz} = -\gamma z$ (z is depth), and again the total vertical stress is independent of time. Hence

$$\frac{\partial\pi}{\partial t} = c_v\,\frac{\partial^2\pi}{\partial z^2} \tag{9}$$

where $c_v = (kE')/(cE' + 1)$ is a consolidation coefficient. If the fluid is incompressible, as is often assumed in soil mechanics, then $c = 0$ and $c_v = kE'$. Equation (9) is the governing equation for the problem in the purely elastic case. However, the form turns out to be the same in the elastic–plastic range of deformation.

Elastic–plastic deformation

Two cases of elastic–plastic deformation are considered. The first is based on the well-known Drucker–Prager criterion; the second is based on the popular Mohr–Coulomb criterion. Both are linear in stress and admit closed-form solutions to the poroelastic/plastic consolidation problem involving settlement of a weightless half-space under a uniform surface load, or equivalently, of an infinitely deep, weightless column under the same surface load but restrained laterally, as shown in Figure 1.

Drucker–Prager plasticity. With adoption of the well-known Drucker–Prager criterion as the plastic potential, the stress–strain relations for the solid skeleton in incremental form ('rules of flow') are

$$\begin{aligned} 0 &= \mathrm{d}\sigma'_{xx} - v\mathrm{d}\sigma'_{yy} - v\mathrm{d}\sigma'_{zz} + \lambda E\,\frac{\partial Y}{\partial\sigma'_{xx}} \\ 0 &= \mathrm{d}\sigma'_{yy} - v\mathrm{d}\sigma'_{xx} - v\mathrm{d}\sigma'_{zz} + \lambda E\,\frac{\partial Y}{\partial\sigma'_{yy}} \\ E\mathrm{d}\varepsilon^{s}_{zz} &= \mathrm{d}\sigma'_{zz} - v\mathrm{d}\sigma'_{yy} - v\mathrm{d}\sigma'_{xx} + \lambda E\,\frac{\partial Y}{\partial\sigma'_{zz}} \end{aligned} \tag{10}$$

where Y is the plastic potential, $Y = J_2^{(1/2)} + A'I_1 - B'$, $J_2 = (1/6)[(\sigma_2 - \sigma_3)^2 + (\sigma_3 - \sigma_1)^2 + (\sigma_1 - \sigma_2)^2]$, $I_1 = (\sigma_1 + \sigma_2 + \sigma_3)$, $\sigma_1, \sigma_2, \sigma_3$ are the major, intermediate and minor (effective) principal stresses (tension is positive), A' and B' are material constants and λ is an unknown function that is subsequently eliminated from consideration.

A failure criterion F signalling the limit to purely elastic deformation may be used that is different from the plastic potential. In such cases the rules of plastic flow are non-associative. Use of the Drucker–Prager criterion allows for plastic dilatation since the volumetric plastic strain increment $\mathrm{d}\varepsilon^{p}_{v} = 3\lambda A'$ (and also for an effect of the intermediate principal stress on failure and

flow). In fact, any pressure-dependent plastic potential implies plastic dilatation. More complicated plasticity theories may be invoked to limit plastic dilatation. One of the simplest alternatives is to use the well-known Von Mises criterion as the plastic potential while retaining the Drucker–Prager criterion as the failure condition. This alternative is accomplished simply by setting A' equal to zero in the Drucker–Prager criterion as the plastic potential while retaining a non-zero value for failure. Another alternative is to simply use different values of the parameters A and A' in the same criterion. According to the Drucker–Prager plastic potential Y,

$$\begin{aligned}\frac{\partial Y}{\partial \sigma'_{xx}} &= \mp\frac{\sqrt{3}}{6} + A'\\ \frac{\partial Y}{\partial \sigma'_{yy}} &= \mp\frac{\sqrt{3}}{6} + A'\\ \frac{\partial Y}{\partial \sigma'_{zz}} &= \frac{\mp 2\sqrt{3}}{6} + A'\end{aligned} \tag{11}$$

The choice of algebraic sign is determined by the mode of failure, that is, whether the vertical stress causes failure in tension (upper sign) or compression (lower sign). The lower sign applies to the consolidation problem.

Symmetry of the problem and isotropy of material imply equality of total horizontal stresses, that is, $\sigma_{xx} = \sigma_{yy} = \sigma_h$, and of the effective stresses as well. In cylindrical coordinates, the condition is $\sigma_{rr} = \sigma_{\theta\theta} = \sigma_h$. The same is true in the case of transversely isotropic materials when the vertical axis is normal to the plane of isotropy. The failure criterion then shows

$$\sigma'_h(2\sqrt{3}A \mp 1) + \sigma'_{zz}(\sqrt{3}A \pm 1) = \sqrt{3}B,$$

that is,

$$\sigma'_h = \frac{\sqrt{3}B - \sigma'_{zz}(\sqrt{3}A \pm 1)}{(2\sqrt{3}A \mp 1)},$$

so

$$d\sigma'_h = K_0 \mathrm{d}\sigma'_{zz} \tag{12a, d}$$

where

$$K_0 = -\frac{(\sqrt{3}A \pm 1)}{(2\sqrt{3}A \mp 1)}$$

and where the lower sign applies to the consolidation problem.

The material constants A and B used in the failure criterion are directly related to strength of the material and differ from A' and B' used in the plastic potential Y when the rules of flow are non-associative. In any case,

$$A = \left(\frac{1}{\sqrt{3}}\right)\left[\frac{C_0 - T_0}{C_0 + T_0}\right] \quad \text{and} \quad B = \left(\frac{2}{\sqrt{3}}\right)\left[\frac{C_0 T_0}{C_0 + T_0}\right] \tag{13}$$

where C_0 and T_0 are the unconfined compressive and tensile strengths, respectively.

Elimination of λ from the first two of equation (10) together with the use of equations (11) and (12) in the third equation of equation (10) shows that

$$E\mathrm{d}\varepsilon_{zz}^{\mathrm{s}} = [1 - 2\nu K_0 + 2\nu K_{\mathrm{p}} - 2(1-\nu)K_0 K_{\mathrm{p}}]\,\mathrm{d}\sigma'_{zz} \tag{14}$$

where

$$K_{\mathrm{p}} = \frac{(\sqrt{3}A' \pm 1)}{(2\sqrt{3}A' \mp 1)} \tag{14a}$$

After integration

$$\varepsilon_{zz}^{\mathrm{s}} = \frac{\sigma'_{zz}}{E'} + \varepsilon_0^{\mathrm{s}} \tag{15}$$

where

$$E' = E_{\mathrm{p}} = \frac{E}{[1 - 2\nu K_0 + 2\nu K_{\mathrm{p}} - 2(1-\nu)K_0 K_{\mathrm{p}}]} \tag{16}$$

is an 'effective' elastic–plastic modulus and $\varepsilon_0^{\mathrm{s}}$ is a constant of integration. When associative flow rules are used $K_{\mathrm{p}} = -K_0$. Use of equation (15) in equation (6) leads to the same governing equation (9), although E' is now a Drucker–Prager elastic–plastic modulus.

Mohr–Coulomb plasticity. With adoption of the famous Mohr–Coulomb criterion as the plastic potential, the stress–strain relations for the solid skeleton in incremental form ('rules of flow') require consideration of the multiple yield surfaces in stress space that constitute a pyramidal yield surface in contrast to the conical Drucker–Prager yield surface. In fact, the equality of horizontal stresses locates elastic–plastic stress points on an edge of the Mohr–Coulomb yield surface. Hence,

$$\begin{aligned}
0 &= \mathrm{d}\sigma'_{xx} - \nu\mathrm{d}\sigma'_{yy} - \nu\mathrm{d}\sigma'_{zz} + \lambda_x E\,\frac{\partial Y_x}{\partial\sigma'_{xx}} \\
0 &= \mathrm{d}\sigma'_{yy} - \nu\mathrm{d}\sigma'_{xx} - \nu\mathrm{d}\sigma'_{zz} + \lambda_y E\,\frac{\partial Y_y}{\partial\sigma'_{yy}} \\
E\mathrm{d}\varepsilon_{zz}^{\mathrm{s}} &= \mathrm{d}\sigma'_{zz} - \nu\mathrm{d}\sigma'_{yy} - \nu\mathrm{d}\sigma'_{xx} + \lambda_x E\,\frac{\partial Y_x}{\partial\sigma'_{zz}} + \lambda_y E\,\frac{\partial Y_y}{\partial\sigma'_{zz}}
\end{aligned} \tag{17}$$

where Y_x is the plastic potential for $\mathrm{d}\varepsilon_{xx}^{\mathrm{p}}$, $Y_x = \tau_m + C'\sigma_m - D'$, $\tau_m = [(1/2)(\sigma'_{zz} - \sigma'_{xx})^2 + (\tau_{zx})^2]^{(1/2)}$, $\sigma_m = (1/2)(\sigma'_{xx} + \sigma'_{zz})$, and similarly for Y_y, C' and D' are material constants and the λ's are unknown functions, subsequently eliminated from consideration.

According to the Mohr–Coulomb plastic potential

$$\begin{aligned}
\frac{\partial Y_x}{\partial\sigma'_{xx}} &= \mp\frac{1}{2} + \frac{C'}{2} \\
\frac{\partial Y_y}{\partial\sigma'_{yy}} &= \mp\frac{1}{2} + \frac{C'}{2} \\
\frac{\partial Y_x}{\partial\sigma'_{zz}} = \frac{\partial Y_y}{\partial\sigma'_{zz}} &= \pm\frac{1}{2} + \frac{C'}{2}
\end{aligned} \tag{18}$$

With $\sigma_{xx} = \sigma_{yy} = \sigma_h$, as before, the failure criterion shows that

$$\sigma'_h(C \mp 1) + \sigma'_{zz}(C \pm 1) = 2D$$

that is,

$$\sigma'_h = \frac{2D - \sigma'_{zz}(C \pm 1)}{(C \mp 1)}$$

so,

$$\mathrm{d}\sigma'_h = K_0 \mathrm{d}\sigma'_{zz}, \tag{19a, d}$$

where

$$K_0 = -\frac{(C \pm 1)}{(C \mp 1)}$$

and where the lower sign applies for compressive failure anticipated in the consolidation problem. The plastic dilatation increment is $\mathrm{d}\varepsilon^{\mathrm{p}}_{\mathrm{v}} = (\lambda_x + \lambda_z)C'$ which is expansive.

The material constants C and D used in the failure criterion are directly related to strength of the material and differ from C' and D' used in the plastic potential Y when the rules of flow are non-associative. In either case,

$$C = \left[\frac{C_0 - T_0}{C_0 + T_0}\right] \quad \text{and} \quad D = \left[\frac{C_0 T_0}{C_0 + T_0}\right] \tag{20}$$

where C_0 and T_0 are the unconfined compressive and tensile strengths, respectively.

Elimination of λ's from the first two of equation (17) together with the use of equations (18) and (19) in the third equation of equation (17) shows that

$$E\mathrm{d}\varepsilon^{\mathrm{s}}_{zz} = [1 - 2vK_0 + 2vK_{\mathrm{p}} - 2(1-v)K_0K_{\mathrm{p}}]\,\mathrm{d}\sigma'_{zz} \tag{21}$$

where

$$K_{\mathrm{p}} = \frac{(C' \pm 1)}{(C' \mp 1)} \tag{222}$$

After integration

$$\varepsilon^{\mathrm{s}}_{zz} = \frac{\sigma'_{zz}}{E'} + \varepsilon^{\mathrm{s}}_0 \tag{23}$$

where $E' = E/[1 - 2v_0 + 2vK_{\mathrm{p}} - 2(1-v)K_0K_{\mathrm{p}}]$ is an elastic–plastic modulus and $\varepsilon^{\mathrm{s}}_0$ is a constant of integration. When associated flow rules are used $K_{\mathrm{p}} = -K_0$, as before. Thus, the form of the elastic–plastic effective stress strain relationship in the z-direction is the same in either case. Again, the governing equation (9) assumes the same form, although E' is now a Mohr–Coulomb elastic–plastic modulus.

Compressive and tensile strengths are convenient in analysis of porous, fractured rock mechanics problems, but the angle of internal friction ϕ and cohesion c' (not to be confused with fluid compressibility used previously) are more convenient in soil mechanics problems. The relations between the various material strength parameters are: $\sin(\phi) = C\sqrt{3A}$ and $c' = D/\cos(\phi) = \sqrt{3B/2}\cos(\phi)$.

Elastic–plastic boundary

The analysis proceeds with the assumption that loading is initially elastic from the unstressed, unstrained state. Application of the applied surface and gravity loads occurs at the zero of time either as a fast ramp load over a small but finite time step or instantaneously as step function. Incremental ramp loading has the advantage of allowing for yielding prior to peak load application and is necessary when the pore fluid is incompressible.

However, yielding may not occur during load application, but instead may follow during the subsequent consolidation phase as drainage proceeds in time and load is transferred from fluid to solid. Thus, while the total applied load may be constant, the effective stresses that determine yielding change with time. In 'dry' elastic–plastic analysis, a monotonic time-like parameter is usually introduced that allows loading to increase with time and yielding to eventually occur. In coupled analyses, real time is involved. Questions intrinsic to elastic–plastic analyses concern first yielding, the spread of the elastic–plastic region and collapse. A proper solution to an elastic–plastic boundary value problem answers these question by expressing the location of the interface between the purely elastic and elastic–plastic regions as a function of the applied loads, which may be time-dependent but are constant in the problem at hand.

The combined problem of surface and gravity loading allows for initial yielding at the column top, bottom (in a column of finite depth) or at some other depth, or both, during loading or later during consolidation. Loading may be a step function in zero time or as ramp requiring a relatively small time step. The latter approach is convenient when the pore fluid is incompressible. The number of possibilities suggests separate discussion for clarity. The first problem involves application of a uniform compressive surface load to an unstressed weightless material; the second involves an initial stress caused by material weight.

With neglect of weight and the assumption of a Poisson's ratio of zero, a uniformly distributed surface load $-\sigma_0$ generates an effective stress that results in yielding when the uniaxial compressive strength is reached, that is, when $\sigma'_{zz} = \sigma_0 - \pi = -C_0$. Because the applied load and fluid stress are negative, first yield occurs where the equality $-\sigma_0 - \pi = -C_0$ is first satisfied, that is, where the 'spread' between total and fluid stress is greatest. Clearly, if the applied load is less than the compressive strength of the material, then yielding never occurs. If $\sigma_0 < -C_0$ then yielding will occur either during loading or subsequently during consolidation. Under step function loading, the initial distribution of fluid stress $\pi(z, 0^+) = \sigma_0/(1 + cE')$. For example, if $c = 3E'$, then $\pi(z, 0^+) = (3/4)\sigma_0$, then yielding will not occur during loading unless $\sigma_0 < -4C_0$, and in general, if $\sigma_0 < -C_0(1 + cE')/cE'$. If yielding is possible during loading, then because of the uniform state of the column, the entire column yields before the total load can be applied. However, if the pore fluid is considered incompressible, then $\pi(z, 0^+) = \sigma_0$, and no yielding is possible during loading. In case yielding does not occur during loading, then at some later time, sufficient load will be transferred from the pore fluid to the solid to cause first yielding. This event occurs where the magnitude of the fluid stress is least which is at the top of the column where the fluid stress is specified to be zero. In fact, there is a discontinuity in fluid stress at time zero, but drainage at the top of the column smooths the jump relatively fast; the effective stress is then greatest near the column top and, at a given depth, increases with time as the pore pressure decays. Thus, in this case, the plastic zone initiates at the column top and spreads downwards. In a column of finite depth, collapse occurs when the plastic zone penetrates to the column bottom.

In the case of gravity loading only and, again, with the assumption of zero Poisson's ratio, the total vertical stress is $-\gamma z$, so yielding is possible when $-\gamma z - \pi = -C_0$. The initial fluid stress

distribution in this example is $-\gamma z/(1+cE') = -(3/4)\gamma z$, while the long-term distribution is simply $-\gamma_f z$ (specific weight of fluid times depth). The greatest spread between total and fluid stress occurs increases with depth, so at some depth ($z = H$), first yielding occurs during the loading period, provided $\gamma H > 4C_0$. In a column of finite depth H, if the spread $(\gamma - \gamma_f)H$ is less than C_0, then yielding never occurs. Otherwise, yielding is initiated at some time at the column bottom, where fluid flow is specified zero. In either case, yielding propagates upwards from depth H until the effective stress becomes numerically less than the unconfined compressive strength of the material.

SOLUTION

The problem requires the following equations to be satisfied:

$$\begin{aligned}
&\frac{\partial \pi_p}{\partial t} = c_p^2 \frac{\partial^2 \pi_p}{\partial z^2} \quad (0 < z < Z(t),\ t > 0)\\
&\frac{\partial \pi_e}{\partial t} = c_e^2 \frac{\partial^2 \pi_e}{\partial z^2} \quad (Z(t) < z < \infty,\ t > 0)\\
&\pi_p = P_1 \quad (z = 0)\\
&\pi_e = P_0 \quad (t = 0+)\\
&\pi_p = \pi_e \quad (z = Z(t))\\
&\frac{\partial \pi_p}{\partial z} = \frac{\partial \pi_e}{\partial z} \quad (z = Z(t))
\end{aligned} \tag{24a–f}$$

where the subscripts p and e refer to the plastic and elastic regions, respectively, and c_p^2 and c_e^2 are consolidation coefficients (c_v's) in the plastic and elastic regions. The square is used for convenience. Equations (24a) and (24b) are just the governing equations in the plastic and elastic regions, equation (24c) is a boundary condition at the surface, equation (24d) is an initial condition, equation (24e) and (24f) express continuity of fluid stress and velocity at the elastic–plastic interface that occurs in time at depth $z = Z(t)$. A discontinuity in pressure occurs at the surface under step function loading. The permeable surface approached from the outside has zero fluid stress ($P_1 = 0$), but has an initial stress when approached from the inside. The initial fluid stress $P_0 = \pi(z, 0^+) = \sigma_0/(1 + cE')$. In the purely elastic case, equations (24b)–(24d) are the applicable equations. Dimensionless variables

$$t^* = \frac{c_v t}{Z^2}, \qquad z^* = \frac{z}{Z}, \qquad \pi^* = \frac{\pi}{\sigma_0}$$

could be used to normalize the governing equations (24), but there is no particular advantage to doing so because of the difference in the consolidation coefficients in the elastic–plastic and purely elastic regions.

Equations (24) define a Stefan problem that has a solution in the form[7–9]

$$\begin{aligned}
Z(t) &= 2\beta\sqrt{t}\\
\pi_p &= P_1 + A\,\mathrm{erf}(z/2c_p\sqrt{t})\\
\pi_e &= P_0 + B\,\mathrm{erfc}(z/2c_e\sqrt{t})
\end{aligned} \tag{25a–c}$$

where erf(·) and erfc(·) are the error and complimentary error functions, respectively.[10] Constants A and B can be determined from the first continuity condition, provided π is known at the elastic–plastic interface. In the purely elastic case $\pi = P_0 \operatorname{erf}(z/2c_e\sqrt{t})$.

Continuity of total stress, fluid stress and effective stress requires that the stresses on either side of the elastic–plastic interface satisfy the failure criterion. This requirement is often used in conventional plasticity analysis to assist in locating the elastic–plastic interface as a function of the external boundary conditions. Hill[11] points out that determining the location of the elastic–plastic interface is central to the solution of many problems in plasticity theory. In the Drucker–Prager case, the continuity requirements lead to

$$\sigma'_{zz} = \frac{-C_0}{1-(v/(1-v))[(3C_0/2T_0)-\frac{1}{2}]} = C_{DP} \tag{26}$$

and, in the Mohr–Coulomb case, to

$$\sigma'_{zz} = \frac{-C_0}{1-(v/(1-v))[C_0/T_0]} = C_{MC} \tag{27}$$

which coincides with C_{DP} in the special case of $v = 0$. The two cases also coincide in the special case of C_0/T_0. In the first special case, the horizontal stress in the elastic region is zero. Equations (26) and (27) then show that initial yielding occurs when the effective stress equals the unconfined compressive strength of the column material, as one would expect. In the second special case, failure is always possible for $v < 0{\cdot}5$. However, the minus sign in the denominator of equations (26) and (27) shows that compressive failure in uniaxial strain is unlikely over a wide range of realistic combinations of Poisson's ratio and ratios of unconfined compressive to tensile strength (σ'_{zz} must be negative).

The fluid stress is just the difference between total and effective stress, so the fluid stress π_{EP} at the elastic–plastic interface is

$$\pi_{EP} = \sigma_0 - C_{DP} \quad \text{or} \quad \pi_{EP} = \sigma_0 - C_{MC} \tag{28a, b}$$

where σ_0 is the uniformly distributed surface load and tension is positive. The required constants are then

$$A = \frac{(\pi_{EP} - P_1)}{\operatorname{erf}(\beta/c_p)}, \qquad B = \frac{(\pi_{EP} - P_0)}{\operatorname{erfc}(\beta/c_e)} \tag{29a, b}$$

The constant β can be found from the second continuity condition that leads to

$$c_e(\pi_{EP} - P_1)\exp(-\beta^2/c_p^2)\operatorname{erfc}(\beta/c_e) = -c_p(\pi_{EP} - P_0)\exp(-\beta^2/c_e^2)\operatorname{erfc}(\beta/c_p) \tag{30}$$

where exp(·) means $e^{(\cdot)}$, Equation (30) is easily solved numerically for the constant β.

Figure 2 shows plots of the left- and right-hand sides of equation (30) for material properties used in an example problem ($\beta = 6{\cdot}706$), for the incompressible fluid case ($\beta = 5{\cdot}589$) and for a case of limiting fluid compressibility being *less* than the elastic modulus of the solid ($\beta = 25{\cdot}570$). The left-hand side of equation (30) is always negative, but it is possible that the right side becomes positive. This change occurs when $(\pi_{EP} - P_0)$ becomes negative. In this case there is no solution to equation (30). The physical reason is that failure of the column then occurs

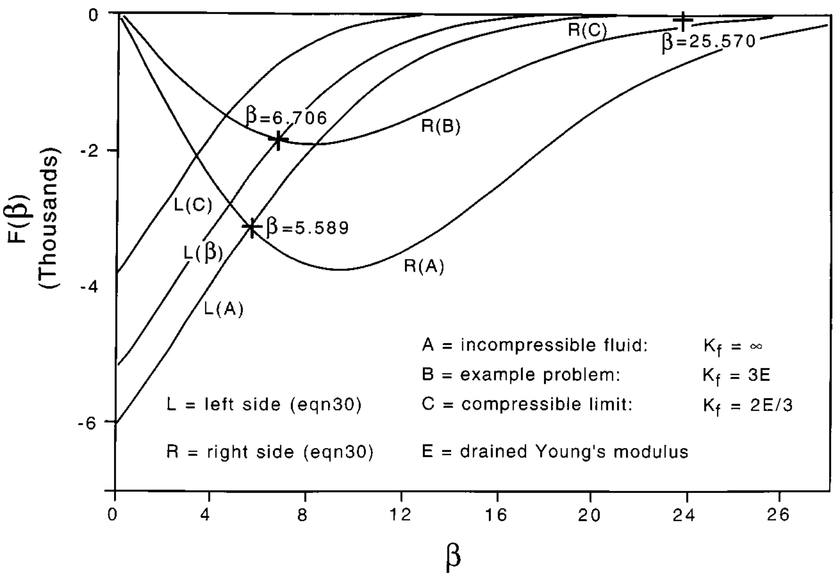

Figure 2. Graphical solution for the parameter beta (β). (a) incompressible pore fluid, (b) fluid less compressible than the solid, (c) fluid more compressible than the solid

instantaneously with loading, contrary to the assumption of failure occurring during subsequent consolidation of the loaded column. In the special case of $v = 0$, failure will not occur instantaneously provided $\sigma_0 - P_0 > -C_0$. This restriction requires the fluid bulk modulus $K_f > E'[(-\sigma_0/C_0) - 1]$ where compression is negative and the assumption of $v = 0$ is made for illustrative purpose. If the elastic and plastic consolidation coefficients in equation (30) are set equal, the result is equivalent to the purely elastic solution for fluid stress at depth $z = Z$.

After substitution of equations (29a) and (29b) into equations (25b) and (25c) and the use of equation (25a) to eliminate t, the solution for fluid stress has the form

$$Z(t) = 2\beta\sqrt{t}$$

$$\pi_p = P_1 + \frac{(\pi_{EP} - P_1)}{\mathrm{erf}(\beta/c_p)}\,\mathrm{erf}[(\beta/c_p)(z/Z)] \tag{31a–c}$$

$$\pi_e = P_0 + \frac{(\pi_{EP} - P_0)}{\mathrm{erfc}(\beta/c_e)}\,\mathrm{erfc}[(\beta/c_e)(z/Z)]$$

where $Z(t)$ is depth to the elastic–plastic interface. This form clearly shows the role of the elastic–plastic interface position in determining the fluid stress in the elastic region and points out the potential for error in simply attempting to match solutions between regions.

Inspection of equations (31b)–(31c) shows that the fluid stress is indeed continuous at the elastic–plastic interface. Differentiation and substitution into equation (24f) leads to equation (30), so the continuity requirement equation (24f) is also met.

Because the total vertical stress is constant in this problem, the effective vertical stress is obtained simply by subtracting the fluid stress from the total stress. The horizontal effective

stresses are obtained from the vertical effective stress using Hooke's law as is the vertical strain in the solid skeleton. In the special case of $v = 0$, the horizontal stresses in the elastic region are zero, as seen immediately from Hooke's law equation (5), but this is not the case in the plastic region, as seen from equations (12) or (19). Interestingly, the horizontal stresses in the plastic region can be calculated, in any case, provided the effective vertical stress is known. This observation allows for a quick check on numerical results obtained, say, from finite element analysis. Thus, the effective stresses in the plastic region ($0 < z < Z(t)$, $t > 0$) are

$$\begin{aligned} \sigma'_{zz} &= \sigma_0 - \pi_\mathrm{p} \\ \sigma'_{xx} &= \sigma'_{yy} = K_0 \sigma'_{zz} \end{aligned} \tag{32a, b}$$

where K_0 is given by either equation (12d) or equation (19d) depending on whether Drucker–Prager or Mohr–Coulomb yield is used. In the elastic region ($Z(t) < z < \infty$, $t > 0$)

$$\begin{aligned} \sigma'_{zz} &= \sigma_0 - \pi_\mathrm{e} \\ \sigma'_{xx} &= \sigma'_{yy} = K_0 \sigma'_{zz} \end{aligned} \tag{33a, b}$$

where $K_0 = v/(1 - v)$.

Displacement in the purely elastic case is obtained by integration of the stress–strain–displacement equation. After the first integration, the time-dependent strain is

$$\frac{\partial w}{\partial z} = \left(\frac{1}{E'}\right)[P_0 - P_0 \operatorname{erf}(z/2c_\mathrm{e}\sqrt{t})] \tag{34}$$

After the second integration, the time-dependent displacement is

$$w(z, t) = \left(\frac{1}{E'}\right)\{P_0 z \operatorname{erfc}(z/2c_\mathrm{e}\sqrt{t}) - 2P_0 c_\mathrm{e}\sqrt{t/\pi}\exp[-(z/2c_\mathrm{e}\sqrt{t})^2]\} \tag{35}$$

The time-dependent surface displacement has a simple expression

$$w(0, t) = \left(\frac{-1}{E'}\right)2P_0 c_\mathrm{e}\sqrt{t/\pi}) \tag{36}$$

These results may be checked by comparison with a previously validated poroelastic finite element code and solution to the analogous problem of finite depth, provided the initial conditions in a region near the bottom of the column have not undergone significant change, say, less than 0·1 per cent of initial values.

The instantaneous displacement $w(z, 0)$ for a column of finite depth H is simply $(1/E')(P_0 - \sigma_0)(H - z)$ which is positive and where $P_0 = \sigma_0/(1 + cE')$ with $E' = E_\mathrm{e}$, provided yielding does not occur during loading, otherwise collapse is instantaneous. The instantaneous displacement is unbounded in the case of an infinite column or half-space.

Integration of the elastic–plastic strain displacement equation leads to the expression

$$\begin{aligned} w(z, Z) = &\left(\frac{1}{E_\mathrm{e}}\right)(P_0 - \pi_\mathrm{EP})z + \left(\frac{1}{E_\mathrm{p}}\right)(\pi_\mathrm{EP})z \\ &- \left(\frac{A}{E_\mathrm{p}}\right)\{z \operatorname{erf}[(\beta/c_\mathrm{p})(z/Z)] + (c_\mathrm{p}/\beta)\frac{Z}{\sqrt{\pi}}\exp[-(\beta/c_\mathrm{p})(z/Z)]^2\} \end{aligned} \tag{37}$$

for the time-dependent displacements in the elastic–plastic region ($0 < z < Z$, $t > 0$) where Z is depth to the elastic–plastic interface, as before, E_e and E_p are the 'effective' moduli (E') in the elastic and plastic regions, respectively. The time-dependent surface displacement is

$$w(0,t) = \left(\frac{-A}{E_p}\right)(2c_p)\sqrt{t/\pi} \tag{38}$$

which is obtained by simply substituting $z = 0$ and $Z = 2\beta\sqrt{t}$ into equation (37). The time-dependent displacement of the elastic–plastic interface is

$$w(Z,t) = \left(\frac{1}{E_e}\right)(P_0 - \pi_{EP})(2\beta\sqrt{t}) - \left(\frac{A}{E_p}\right)(2c_p)\sqrt{t/\pi}\exp[-(\beta/c_p)^2] \tag{39}$$

which is obtained by substituting $z = Z = 2\beta\sqrt{t}$ into equation (37).

The time-dependent displacement in the elastic region below the elastic–plastic interface is also obtained by integrating the stress–strain–displacement equation and requiring continuity of displacement at the elastic–plastic interface. The strain is also continuous at the elastic–plastic interface. In the elastic region ($Z < z < \infty$, $t > 0$),

$$\begin{aligned} w(z,Z) = w_p(Z,Z) &+ \left(\frac{1}{E_e}\right)(\pi_{EP} - P_0)Z - \left(\frac{Bz}{E_e}\right)\operatorname{erfc}[(\beta/c_e)(z/Z)] \\ &+ \left(\frac{B}{E_e}\right)\left(\frac{ZC_e}{\beta\sqrt{\pi}}\right)\exp[-(\beta z/c_e Z)^2] - \exp[-(\beta/c_e)^2] \end{aligned} \tag{40}$$

where w_p is given with the substitution of $\sqrt{t} = Z/2\beta$ into the right hand side of equation (39). Equation (40) reduces to $w(Z,Z) = w_p$ at $z = Z$, as required by continuity of displacements.

EXAMPLE RESULTS

An example problem using a Drucker–Prager yield criterion and associated flow rules illustrates the behaviour of a weightless column of infinite depth that consolidates under a uniform compressive surface load. The material properties are taken, in part, from Ghaboussi and Wilson,[4] who examined poroelastic consolidation in a soil-like column saturated with a compressible fluid. Thus

Young's modulus (drained)	$E = 690$ MPa (10,000 psi)
Poisson's ratio (drained)	$\nu = 0$
Fluid bulk modulus	$K_f = 2{\cdot}07$ GPa (30,000 psi)
Effective stress coefficient	$\alpha = 1{\cdot}0$
Hydraulic conductivity	$k = 0{\cdot}003$ m/day (0·01 ft/day)
Elastic consolidation coefficient	$c_e^2 = 16{\cdot}1$ m^2/day (173 ft^2/day)
Elastic–plastic coefficient	$c_p^2 = 14{\cdot}7$ m^2/day (158 ft^2/day)
Unconfined compressive strength	$C_0 = 4{\cdot}14$ MPa (600 psi)
Tensile strength	$T_0 = 1{\cdot}38$ MPa (200 psi)
Cohesion (Mohr–Coulomb yield)	$c' = 1{\cdot}19$ MPa (173 psi)
Angle of internal friction	$\phi = 30^\circ$
Drucker–Prager intercept	$B' = 1{\cdot}19$ MPa (173 psi)
Drucker–Prager slope	$A' = 0{\cdot}289$

The last four properties are derived from the unconfined tensile and compressive strengths. The assumed strengths are high for soils but low for intact rock samples. The ratio of compressive to tensile strength is also unrealistic for rock where tensile strength is generally in the range of 5–10 per cent of the unconfined compressive strength. In many instances the failure envelope of rock and soil is curved and shows a rounded nose in the tensile strength region. However, farther into the region of compressive stress there is a tendency towards linearity. By using the slope ($\tan\phi$) of the envelope in this region and unconfined compressive strength (C_0) to characterize the material, artificially high values of cohesion and tensile strength are generated by the assumed linear failure criterion. The hydraulic conductivity is reasonable for a sand-like material, while the consolidation coefficients are high relative to clay-like material. A Poisson's ratio of zero is a numerical convenience because it readily allows for verification of yielding or failure when the vertical effective stress reaches a value of 4·14 MPa (600 psi) in compression. Because the initial effective stress is only a 1·72 MPa (250 psi) compression under the applied surface compression of 6·90 MPa (1000 psi), initial yielding does not occur instantaneously, but rather during the subsequent consolidation stage. A lower applied stress and lower, more realistic soil strengths could be used in the example calculations. The numerical results would change but the essential features of the analysis would not. Thus, there is some physical justification for using the specified material properties, but they also serve a convenient numerical purpose.

In this example problem, the small numerical difference between consolidation coefficients in the elastic and elastic–plastic domains indicates that the differences between purely elastic and elastic–plastic results for pore fluid pressure and surface displacement should also be small. Indeed, this is the case; the largest difference between the two occurs in the horizontal stress distribution. Of course, there is also the motion of the elastic–plastic boundary to consider.

The distribution of pore fluid pressure with respect to depth at various times is shown in Figure 3. Also shown in Figure 3 are finite element results obtained from a mesh of 1000 elements 0·3 m by 0·3 m (1 ft by 1 ft) in a column 305 m (1000 ft) deep. Pore pressure change does not

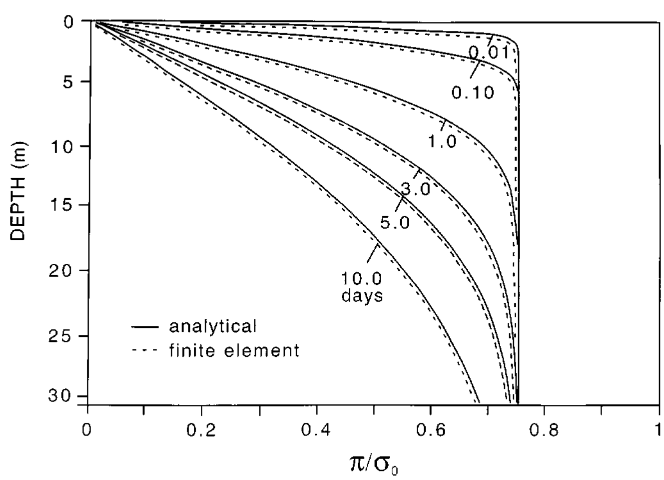

Figure 3. Pore fluid pressure distribution to a depth of 30 m as a fraction of the applied surface load at various times (days)

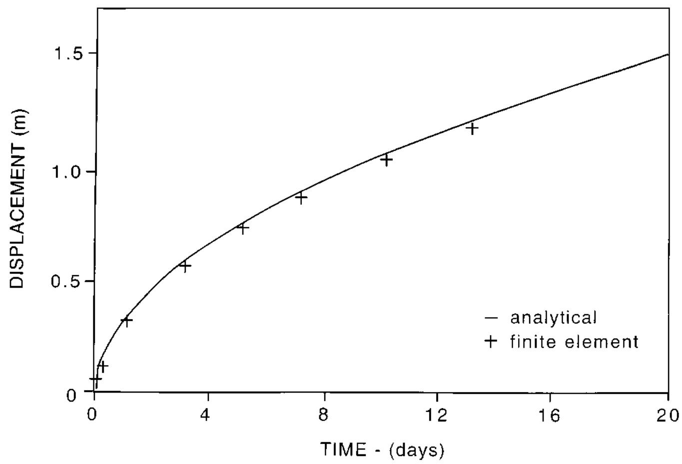

Figure 4. Time-dependent surface displacement

penetrate the column beyond 30 m (100 ft) at the early times. At the latest time (10 days), the change in pore fluid pressure is less than 0·1 per cent of the initial pressure below 56 m (185 ft). The analytical (solid lines) and finite element (dashed lines based on 100 data points) results are in quite close agreement. In fact, they overlap on the original plot and are separated in Figure 3 only to show both results.

The time-dependent surface displacement is shown in Figure 4. The finite element results slightly underestimate surface displacement. The analytical results show that the surface displacement is directly proportional to $\sqrt{t}$ even as the elastic–plastic region deepens. Figure 5 shows the depth to the elastic–plastic boundary as a function of time. The shape of the curves in Figures 4 and 5 is not coincidental. In fact the surface displacement is directly proportional to the depth $Z(t)$ to the elastic–plastic boundary. This observation again emphasizes the fact that locating the elastic–plastic boundary in terms of the external boundary and initial conditions is at the heart of elastic–plastic analysis.

Consolidation is slightly slower in the elastic–plastic case because of the smaller consolidation coefficient. The reason may also be attributed to plastic dilatation. Non-associated flow rules that use a dilatation angle that is smaller than the angle of internal friction would affect this result. The analytical solution allows for an evaluation of the effect without the need for time-consuming, parametric finite element analysis. The effect is quantified in the effective elastic–plastic modulus $E_p = E'$. For example, if the dilatation angle is zero while other properties remain the same, then $E_p = 138$ MPa (20,000 psi) and $c_p^2 = 25{\cdot}8$ m/day (278 ft^2/day) which is greater than c_e^2. Hence, in this case of non-associated plasticity, consolidation in the elastic–plastic region would proceed more rapidly than in the elastic region.

An interesting question that arises is how a material with a compressive strength of 4·14 MPa (600 psi) can remain in equilibrium under a surface load that eventually obtains a value of 6·90 MPa (1000 psi). The answer can only be that the material strength must increase in proportion to the increasing effective stress in the solid skeleton that occurs as the pore fluid pressure diminishes in time. Such an increase in strength is possible provided the effective confining pressure is increased, that is, provided the horizontal stress in the elastic–plastic zone

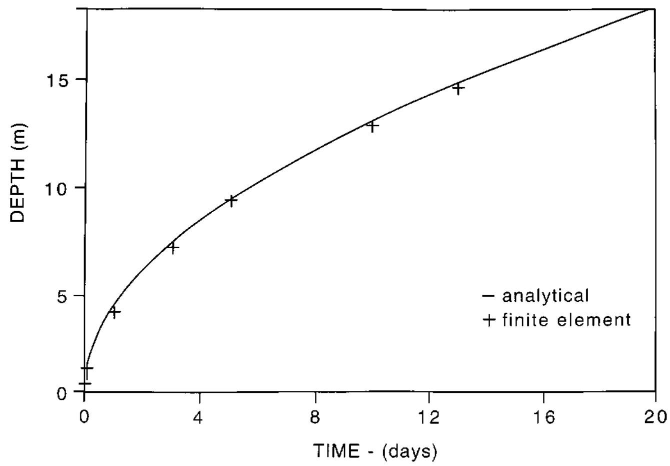

Figure 5. Depth to the elastic–plastic boundary as a function of time

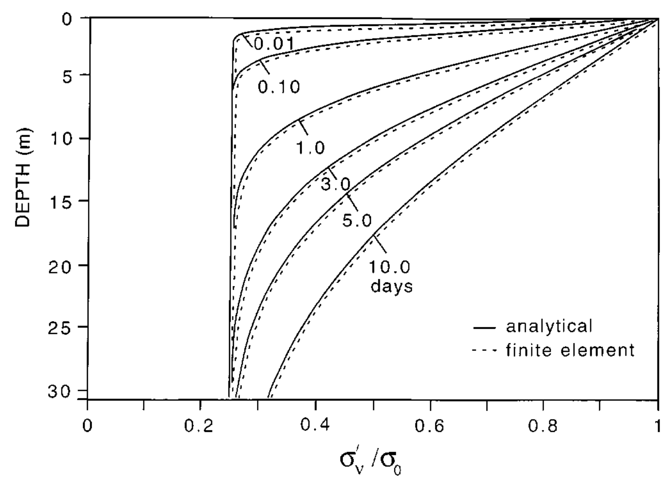

Figure 6. Distribution of effective vertical stress as a fraction of the total applied stress at various times

increases in just the amount needed to increase the compressive strength as required for equilibrium. Strain hardening without mean stress dependent strength (von Mises failure) may respond similarly. Although the horizontal effective stress is zero in the elastic region because Poisson's ratio is assumed to be zero, the horizontal effective stress is not and cannot be zero in the elastic–plastic region where, associated or not, $\sigma_h' = K_0(\sigma_0 - \pi + C_0)$. Figure 6 shows the distribution of vertical effective stress with depth at various times. A vertical line of normalized unconfined compressive strength intersects the curves in Figure 6 at the elastic–plastic boundary. The elastic region is below an intersection point; the elastic–plastic region is above. Figure 7 shows the corresponding distribution of horizontal effective stress with depth. The depth to the

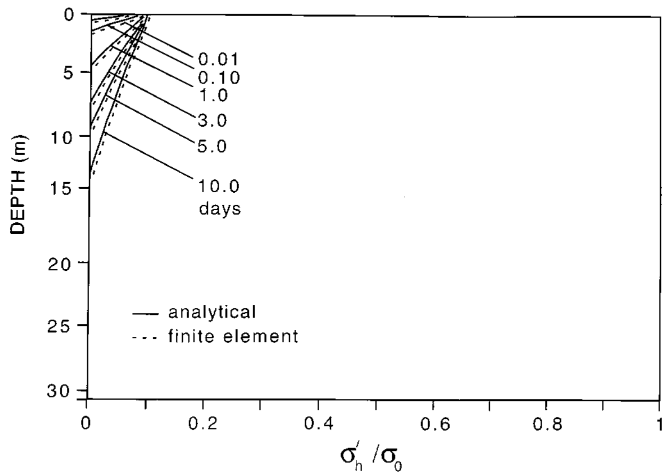

Figure 7. Distribution of effective horizontal stress as a fraction of the applied stress at various times

elastic–plastic boundary in Figure 7 occurs where the curves intersect the vertical axis (zero stress).

CONCLUSION

An analytical solution to the problem of poroelastic/plastic consolidation was obtained using Drucker–Prager (D–P) and Mohr–Coulomb (M–C) criteria. Rules of flow may be non-associative, but must be linear. Integration of the elastic–plastic stress–strain relations results in a form similar to the purely elastic case. The difference is in the 'effective modulus'. However, the same steps taken in the elastic case that reduce the problem to solution of the diffusion equation for pore fluid pressure also suffice for the elastic–plastic case. A noteworthy difference between the two occurs in the consolidation coefficient. In consideration of boundary conditions and initial conditions on pore fluid pressure immediately after application of load, the elastic–plastic pore fluid pressure problem is shown to be equivalent to a classic Stefan ('moving boundary') problem for which the solution is known. Once the time-dependent pore fluid pressure distribution is known, distributions of effective stress are readily obtained as are strains and fluid velocities. Integration of the strain dependent equation then leads to the time-dependent displacement distribution. All distributions may be considered as functions of time or of depth to the elastic–plastic boundary which appears first at the column surface and subsequently moves down the column. Distance to the elastic–plastic boundary is often used as a proxy for real time in time-independent plasticity problems. In this problem, the two are related by the simple expression $Z = 2\beta\sqrt{t}$ where β is a constant determined from continuity conditions at the elastic–plastic boundary.

Validation of poroelastic/plastic finite element codes using D–P and M–C criteria are possible and is one of the main practical uses of the analytical solution. In fact, finite element results are in excellent agreement. Although the analytical solution pertains to a column of infinite depth, results may be applied to columns of finite depth provided the initial pore fluid pressure at the

column changes very little over the comparison time interval. In this regard, a Fourier series solution exists for poroelastic consolidation of columns of finite depth, but not in the poroelastic/plastic case. The analytical solution also allows one to evaluate effects of material property changes on time-dependent surface displacement and so on without the need for costly parametric study by numerical methods.

ACKNOWLEDGEMENT

This research has been supported by the Department of Interior's Mineral Institute program administered by the Bureau of Mines through the Generic Minerals Technology Center in Mine Systems Design and Ground Control under grant number G1145251.

REFERENCES

1. K. Terzaghi, *Theoretical Soil Mechanics*, Wiley, New York, 1943.
2. M. A. Biot, 'General theory of three-dimensional consolidation', *J. Appl. Phys.* **12,** 155–164 (1941).
3. R. S. Sandhu and E. L. Wilson, 'Finite-element analysis of seepage in elastic media', *J. Engng. Mech. Div. EM3*, *Proc. Amer. Soc. Civil Engrs*., 1969, pp. 641–652.
4. J. Ghaboussi and E. L. Wilson, 'Flow of compressible fluid in porous elastic media', *Int. J. Numer. Meth. Engng*., **5,** 419–442 (1973).
5. E. Detournay and A. H.-D. Cheng, 'Fundamentals of poroelasticity', *Comprehensive Rock Engineering*, Vol. 2, Pergamon, New York, 1993, pp. 113–171.
6. W. G. Pariseau, 'Poroelastic settlement of hydraulic fill', *Int. J. Rock Mech. Mng. Sci. Geomech. Abstr*., **25**(2)**,** 255–259 (1998).
7. H. S. Carlsaw and J. C. Jaeger, *Conduction of Heat in Solids*, 2nd edn Clarendon Press, Oxford, 1959, p. 510.
8. L. I. Rubenstein, *The Stefan Problem*, American Mathematical Society, Providence, RI, 1971, p. 419.
9. M. N. Ozisik *Heat Conduction*, Wiley, New York, 1980, p. 687.
10. M. Abramowitz and I. A. Stegun, *Handbook of Mathematical Functions*, Dover, New York, 1965.
11. R. Hill, *The Mathematical Theory of Plasticity*, Clarendon Press, Oxford, 1950, p. 355.

